

Lightness constancy: from haze illusion to haze removal

Cheng Li (李 成)^{1*}, Jianzhong Wang (王建忠)¹, Qingshun Han (韩清顺)¹, and Duyan Bi (毕笃彦)²

¹Aviation University of Air Force, Changchun 130022, China

²Engineering College of Air Force Engineering University, Xi'an 710038, China

*Corresponding author: ecm-li@163.com

Received March 15, 2012; accepted April 13, 2012; posted online June 15, 2012

The human visual system processes lightness constancy to estimate reflectance under complex viewing conditions. We focus on the underlying reason the human visual system is conscious of haze, and discuss the single-image haze-removal problem based on lightness constancy from the beginning of haze illusion. Following the basic principle and model of “atmospheric transfer function”, we bring about a simple dehazing paradigm by estimating two values using bilateral filtering. Practical investigation of parameters and design are analyzed in detail. Furthermore, a novel quantitative standard haziness presents itself naturally during the estimation process. Comparative study and objective evaluation demonstrate that the proposed method is fast and effective, yielding high-contrast and vivid haze-free images.

OCIS codes: 100.0100, 100.2980, 330.1720.

doi: 10.3788/COL201210.081001.

Although not obvious to us, the fact remains that, when we look at a gray surface, such as a blackboard, in outdoor sunlight, the object will appear as gray as it would appear indoors. We know the object should have different luminances under different lighting conditions; however, its appearance does not seem to change to our eyes. This common visual phenomenon is termed as lightness constancy. Experiments have revealed that the human visual system (HVS) is not merely a single “camera” that takes in the actual scene, but a remarkable apparatus with the ability to discount illumination and other viewing conditions, and to estimate the underlying reflectance^[1–3]. Lightness perception involves both the retina and the brain, and this process is subject to illusions, such as the well-known simultaneous contrast effect. These illusions are sometimes viewed as strange failures of visual perception; however, they help reveal the inner mechanism of HVS for achieving lightness constancy.

We find interest in one of these lightness illusions, haze illusion, and derive a possible solution for haze removal. As one of the current hot topics in image-processing field^[4–9], techniques for haze removal have received much attention in remote sensing systems and intelligent vehicles, which are subject to weather conditions. Many investigations have been conducted based on the physical haze-formation model; however, very little attention has been given to its visual characteristics. The proposed priors and assumptions do not provide the essential bases for HVS haze perception. Modeling of human visual characteristics would be beneficial to many engineering fields. For example, for visual computing tasks, we attempt to seek the point of lightness constancy to identify the relationship between the haze model design and scientific interpretation based on HVS in order to advance this field.

Adelson made a precise analysis of lightness perception and light illusions in Ref. [1], defining “atmosphere” as the net effect of viewing conditions (e.g., illuminance, scattering, glare, among others), including additive and multiplicative effects. Human lightness constancy refers to the ability, to some degree, to inverse the atmospheric

transfer function (ATF) that maps reflectance into luminance. The equation of ATF^[1] is

$$L(x, y) = m(x, y)R(x, y) + e(x, y), \quad (1)$$

where L and R are luminance and reflectance of the scene at the pixel (x, y) , respectively, and m and e represent the multiplicative and additive effects, respectively. Different types of atmosphere related with different ATFs lead to different ordinal categories of the X-junction^[1]. The single-reversing X-junction can easily create a hazy atmosphere with an output luminance range compressed by m and shifted up by e . In this letter, we redesign the gray levels, as illustrated in Fig. 1. The labels (1) to (4) in Fig. 1 represent the same gray level, whereas the dashed line represents ATF by Eq. (1).

Figure 2 shows the haze illusion using single-reversing

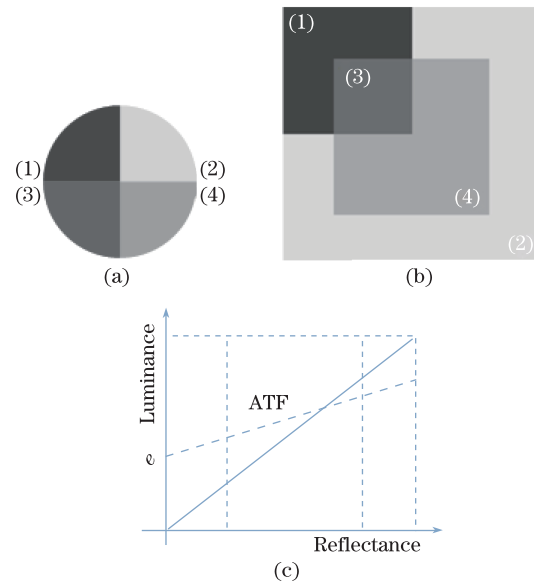


Fig. 1. Formation of hazy atmosphere based on ATF. (a) Single-reversing X-junction, (b) haze illusion, and (c) corresponding ATF diagram.

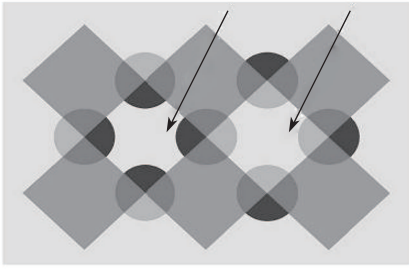


Fig. 2. Typical haze illusion from Adelson^[1]. Regions indicated by arrows obtain the same gray level.

X-junctions to make haze perceptible. The center of the right subregion (arrow) seems visible through the haze, whereas the left one seems to lie in clear air. These regions have the same gray level; however, we can see the differences, especially those induced by the corners. Clark also remarked on the impression of an intentional inexistence between the surface and human vision^[10].

Haze removal is promoted by further progress in image-processing and computational photography tasks. Two basic techniques, image enhancement and image restoration, are used in this research field. The Retinex theory and model have inspired a wide range of developments in haze removal, and estimation of reflectance has been realized by multi-scale retinex with color restoration (MSRCR)^[11] and partial differential equation (PDE) methods^[12]. Recently, single-image haze-removal methods have been proposed with strong priors and assumptions. The starting point is the Koschmieder's haze formation model (HFM)^[4]:

$$I(x, y) = t(x, y)J(x, y) + [1 - t(x, y)]A(x, y), \quad (2)$$

where the equation is defined on RGB space; and I, J, A , and t stand for observed intensity, scene radiance (the objective intensity without haze), global atmospheric light, and medium transmission, respectively.

The goal of haze removal is to recover J from I . Fattal assumed J and t to be locally independent^[4]; however, this physically based method failed when affected by dense fog. Tan^[5] recovered visibility by maximizing the contrast in a local patch, which often led to halo effects. He *et al.*^[6] presented the simple and effective dark channel prior (DCP) based on observation on haze-free images. However, the soft matting procedure had a computational cost, and the necessary post-processing exposure adjustment was only brushed lightly, leaving uncertainty. Tarel^[7] proposed a fast visibility restoration method for practical usage, which needed further refinement of parameters and dynamic range adjustment. Other studies have also been conducted^[8,9].

People often wonder why and how the HVS is subject to haze perception. Part of the answer is provided by the haze illusion. From above, the HFM is merely an application scenario in the general ATF. Much more important is the inverse function of ATF, called "lightness transfer function" (LTF) by Adelson^[1], which provides a clear and definite the solution for avoiding haze illusion and realizing haze removal. In short, to achieve the task of "lightness constancy," we need to figure out R .

Obtaining the prior knowledge of distributions of (e, m)

parameterization would be infeasible, especially because LTF is subjective. We have to rely on the statistical estimation, and deem that an adequate number of pixels in an adaptive window and useful observations will serve us well for better estimation of the LTF mapping.

For a sliding patch Ω in the image $L(M \times N)$, we write the LTF from Eq. (1) as

$$R_{\Omega} = \frac{L_{\Omega}(p) - e_{\Omega}(p)}{m_{\Omega}(p)}, \quad (3)$$

$$L_{\Omega}(p) \in [L_{\Omega \min}, L_{\Omega \max}], R_{\Omega}(p) \in [R_{\Omega \min}, R_{\Omega \max}],$$

where p is the center pixel in the patch. Through anticipated normalization, we can easily illustrate above statement in Fig. 3 (because of the symmetry between ATF and LTF, we still follow on the previous ATF sketch for illustration), labelling the special areas and intervals that are of concern.

Estimating e is a central task of haze removal. First, we derive such two constraints expediently from Fig. 3,

$$\begin{aligned} 0 &\leq e_{\Omega}(p) \leq L_{\Omega \min} \\ 0 &\leq m_{\Omega}(p) \leq 1 \end{aligned} \quad (4)$$

The slope of the ATF m_{Ω} in a patch must take on a positive number and cannot exceed 1 because it is restricted by the linear relationship between L and R . It is also a useful alternative that the white-point (viz. 1) and the black-point (viz. 0) map to the maximum and minimum of R .

Very simply, we can set $e_{\Omega}(p) = L_{\Omega \min}$, which we find relates to the dark channel prior (DCP)^[6] naturally. In other words, DCP can realize estimation of e locally. However, the low intensity in the local region of the original DCP is not practical, because it brings about the block effect and needs computationally intensive soft matting refinement.

In fact, the first expression in Eq. (4) is equivalent to

$$e_{\Omega}(p) = L_{\Omega \min} - \delta_{\Omega}(p), \quad (5)$$

where δ is a small value. Because we have $m_{\Omega} = (L_{\Omega \max} - e_{\Omega}) / R_{\Omega \max}$, *s.t.* $L_{\Omega \max} \leq R_{\Omega \max} \leq 1$, we can introduce another additive factor η to estimate $R_{\Omega \max}$, which leads to

$$m_{\Omega}(p) = [L_{\Omega \max} - e_{\Omega}(p)] / [L_{\Omega \max} + \eta_{\Omega}(p)]. \quad (6)$$

Based on ATF, estimation of (e, m) is based on the (δ, η) . Many filtering methods can be used to obtain a smooth image and the corresponding detailed information. Because we often assume that the statistical sliding window has soft edges, Gaussian convolution is popular operation to form the scale space. However, to per-

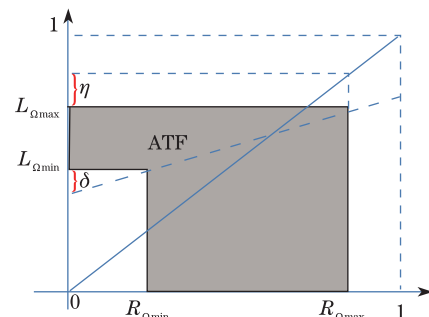


Fig. 3. ATF in a local patch for haze removal.

form the edge-preserving smoothing, we apply bilateral filtering. The whole formula of estimating (δ, η) is inferred as

$$\begin{cases} \delta_{\Omega}(p) = |L_{\Omega \min}(p) - L_{\Omega \min}^{\text{BF}}(p)| \\ \eta_{\Omega}(p) = |L_{\Omega \max}(p) - L_{\Omega \max}^{\text{BF}}(p)| \end{cases}, \quad (7)$$

where $L_{\Omega \min}^{\text{BF}}, L_{\Omega \max}^{\text{BF}}$ is the bilateral filtering result of $L_{\Omega \min}, L_{\Omega \max}$.

Mapping to $[0, 255]$ is always the last step to obtain the output image in display; therefore, other multiplicative factors can be naturally reduced, which saves much more effort.

The visual system adjusts an adaptive window to estimate the lightness mapping^[1]. Simulating this ability is extremely difficult; thus, we design an alternative method to obtain the adaptive adjacency based on local relativity. Although local operation based on a sliding window often leads to the halo effect and other artifacts, we can shrink the window down to one pixel to carry out the minimization value of color channels, that is,

$$L_{\Omega \min} = \min(L_c), L_{\Omega \max} = \max(L_c), c \in \{r, g, b\}. \quad (8)$$

The bilateral filtering is performed by a sliding window whose size is related to the size of image. Two neighboring operations are combined for better performance. For robustness and pleasing perspective based on the experience of estimating transmission map^[6], we also introduce a scaling parameter γ to adjust e and m . Such a nonlinear modification obtains the property that we restrict the maximum value of (e, m) and adaptively keep additional haze for the distant objects. In addition, our method can handle gray-level images. For a gray-scale image, the default window size for calculating $L_{\Omega \min}$ and $L_{\Omega \max}$ is set as 3×3 to avoid the single-channel comparison problem.

For better visualization, many studies introduce pre-processing (e.g., white balance in Ref. [7]) and post-processing (e.g., gamma adjustment in Ref. [7]), or other image enhancement techniques (unaccounted in Ref. [6]). These approaches are all very useful and necessary for complex imaging and display conditions. However, the algorithm had better contain less of these techniques for conciseness and validity.

We must compute an indicator to measure the haze. Based on the proposed method, we define haziness as

$$h = \sum_{\Omega \in L} e_{\Omega}(p)[1 - m_{\Omega}(p)]/MN, \quad (9)$$

where, for an image L , the accumulation of the responding $e(1-m)$ of each pixel represents the density of the haze in the scene. The bigger value of e and the smaller value of m in ATF lead to worse lightness constancy and denser haze.

Furthermore, we can reuse our method to make quantitative evaluation of different haze removal methods. If the restored haze-free image by a certain method serves as the input image, the responding new h (called h_{de}) and the output could act as tokens. A smaller value of h_{de} implies that the restored image has less haziness, thereby better validating the performance of the dehazing method. Haze-free images using dehazing approaches

of good performance must have the most similarity and the closest value of h_{de} . Thus, h_{de} tests the robustness of different algorithms.

Evaluating the visibility from the hazy images, we compare results subjectively and objectively using typical testing images in literature. The most computation-expensive convolution of bilateral filtering is performed by sliding window and accumulation. Typical parameters are size of the sliding window sw is $2 \times \text{floor}[\max(M, N)/100] + 1$, spatial sigma σ_d is $\max(M, N)/30$, and range sigma σ_r is 0.1. The default adjusting parameter γ is 0.90. Because our idea for carrying out the ATF is very simple and does not apply any pre- or post-processing steps, a standard PAL image of 640×480 takes less than 3 s by Matlab2008 on a PC with 2.26 GHz Intel Duo CPU. Clearly, the time spent is much less than in previous methods (e.g., Refs. [4–9]).

Display conditions on screen settled by graphical chipset and software may lead to different visual performance (e.g., color adjustment); however, haze perception is less. Qualitative comparisons of results by popular methods and the proposed one are shown in Figs. 4 and 5. Our results are similar to those of the past models, and have better performance in some aspects. In Fig. 4, the haze dispersed in green leaves and red bricks is

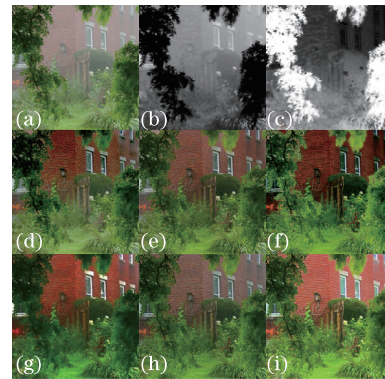


Fig. 4. Typical testing and comparison. (a) Original image^[4], (b) estimation of e , (c) estimation of m , results obtained by (d) Fattal^[4], (e) He^[6], (f) Tarel^[7], (g) Chu^[8], (h) Zhang^[9], and (i) our algorithm.

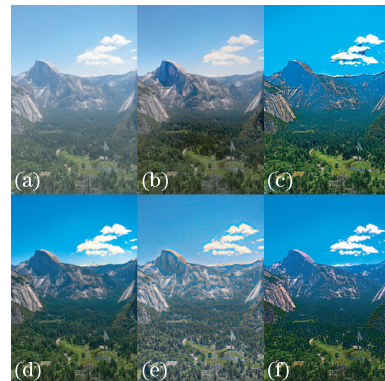


Fig. 5. Typical testing and comparison. (a) Original image^[7], results obtained by (b) Fattal^[4], (c) Tan^[5], (d) He^[6], (e) Tarel^[7], and (f) our algorithm.

hard to remove; however, our haze-free image is much more visually pleasing because of the good estimation of e and m . Other methods reveal shortcomings to some degree, which may introduce oversaturation (Fig. 4(g)), or cannot remove haze sufficiently (Fig. 4(d-h)). In Fig. 5, our result has better contrast and vivid color for a natural scene in damp haze; however, it does not introduce too much halo-effect, such as in Fig. 5(c), and removes the haze sufficiently. More haze-free results are shown in Fig. 6, demonstrating that our algorithm is suitable for many different hazy image conditions.

Based on the haziness, we assess the above results objectively with the corresponding values in Table 1. Clearly, the values of haziness are much reduced after the dehazing, which proves the validity of haze-removal methods and visual restoration of haze-free images.

In conclusion, we present a simple paradigm using estimation and filtering. We believe that the more important task is the modeling of human visual characteristics to produce a wonderful solution for image-processing tasks, in addition to perfecting intuition from seeing combined by exquisite doing. Certainly, just for the powerful ability of HVS, some deficiencies remain evident from our results, such as color-shift and faintness. Methods can be re-



Fig. 6. (b), (d), (f), (h), (j) are haze removal results of original images of (a), (c), (e), (g), (i). (Figs. (a) (e) are from Ref. [5], (c), (g) and (i) are from Ref. [6].).

Table 1. Haziness of Images before and after Haze Removal

Image	Haziness	Image	Haziness
Fig. 4(a)	0.16093	Fig. 4(d)	0.043473
		Fig. 4(e)	0.045834
		Fig. 4(f)	0.001028
		Fig. 4(g)	0.023810
		Fig. 4(h)	0.054514
Fig. 4(i)	0.013772	Fig. 4(j)	0.013772
		Fig. 5(a)	0.22820
		Fig. 5(b)	0.153260
		Fig. 5(c)	0.023836
		Fig. 5(d)	0.060782
Fig. 5(e)	0.113430	Fig. 5(f)	0.028704
		Fig. 6(a)	0.37272
		Fig. 6(b)	0.079333
		Fig. 6(c)	0.17120
		Fig. 6(d)	0.033627
Fig. 6(e)	0.32753	Fig. 6(f)	0.094561
		Fig. 6(g)	0.21462
		Fig. 6(h)	0.032495
		Fig. 6(i)	0.20096
		Fig. 6(j)	0.045952

designed from the view of variational energy function or sparse representation, which could mathematically lead to better estimation and calculation of the ATF. For display, further pre- and post-processing would be useful, especially for images using the *.jpg format. Modeling of the lightness constancy in Eq. (1) needs further study with regard to HVS, including various interesting illusions. The degradation of imaging because of weather conditions prompts us to seek several specialized methods, not an all-purpose one.

This work was supported by the Aeronautical Science Foundation of China under Grant No. 20101996009.

References

1. E. H. Adelson, *Lightness Perception and Lightness Illusions* (The New Cognitive Neurosciences, 2nd ed., M. Gazzaniga, ed. MIT Press, Cambridge, 2000).
2. M. Ebner, *Color Constancy* (John Wiley & Sons Ltd, England, 2007).
3. L. Tao and G. Xu, *Chin. Sci. Bull.* **46**, 1411 (2001).
4. R. Fattal, in *Proceedings of ACM Trans.* **27**, 72 (2008).
5. R. T. Tan, in *Proceedings of IEEE Computer Vision and Pattern Recognition 1* (2008).
6. K. He, J. Sun, and X. Tang, in *Proceedings of IEEE Computer Vision and Pattern Recognition 1956* (2009).
7. J. P. Tarel and N. Hautiere, in *Proceedings of IEEE International Conference on Computer Vision 2201* (2009).
8. C. T. Chu and M. S. Lee, in *Proceedings of PCM 2010 350* (2010).
9. J. Zhang, L. Li, G. Yang, Y. Zhang, and J. Sun, *Vis. Comput.* **26**, 761 (2010).
10. A. Clark, in *Proceedings of University of Pennsylvania Workshop on Cognitive and development factors in Perceptual constancy 1* (2009).
11. D. J. Jobson, Z. Rahman, and G. A. Woodell, in *Proceedings of IEEE Trans. Image* **6**, 451 (1997).
12. C. Li, S. Gao, and D. Bi, *Chin. Opt. Lett.* **7**, 784 (2009).